

Wideband Scattering Performance of Reflectarray Using Log-periodic Dipole Array

Hiroki Ito *Nonmember*, Keisuke Konno *Member, IEEE*, Hiroyasu Sato *Member, IEEE*, and Qiang Chen, *Senior Member, IEEE*

Abstract—In this letter, wideband scattering performance of a reflectarray composed of a log-periodic dipole array (LPDA) is designed and studied numerically and experimentally. The reflectarray is designed using method of moments (MoM). Numerical simulation demonstrates that a reflectarray composed of the LPDA is wideband because the LPDA works as a wideband reflectarray element due to its self-complementary structure. The reflectarray is fabricated using a 3D printing technology, and its scattering performance is experimentally confirmed. Finally, it is shown that the 1-dB and 3-dB bandwidths of the designed reflectarray are 45 % and 64%, respectively.

Index Terms—Reflectarray, Log-periodic dipole array, 3D printing technology

I. INTRODUCTION

A reflectarray is well known as a scatterer that can scatter an incident wave in a specific direction [1]. The first reflectarray that was proposed in [1] uses a rectangular waveguide as its element; this reflectarray is bulky and heavy. To overcome these disadvantages, planar reflectarrays composed of a microstrip array element have been proposed [2], [3]. Planar reflectarrays have numerous advantages compared with the conventional waveguide reflectarray, specifically, flatness, compactness, and easy fabrication. Therefore, various planar reflectarrays have been developed for specific applications such as satellite [4], [5] and wireless communications [6], [7].

The most severe drawback of planar reflectarrays is the narrow bandwidth. The bandwidth of a planar reflectarray is limited by two factors. The first is the inherent narrow bandwidth of planar reflectarray elements. The second is the differential spatial phase delay, resulting from different path lengths between a primary source and each reflectarray element. To overcome the narrow bandwidth of planar reflectarrays, various remedies have been proposed. A multilayer reflectarray was proposed to enhance the bandwidth of planar reflectarrays [8], [9]. Wideband or dual-band loop elements and an I-shaped element have been proposed [10]-[14]. To the best of our knowledge, the 3-dB bandwidth of such wideband reflectarrays ranges from 10% to 30 %.

In recent years, various multiband or wideband reflectarrays have been proposed. An FSS backed circularly polarized reflectarray has been proposed as a satellite communication

antenna [15]. The proposed reflectarray has multiband performance because the FSS works as a ground plane for the Ka band, while the FSS is transparent for the L band. A wideband folded reflectarray operating at 11-15 GHz has been proposed [16]. The folded reflectarray is composed of a novel wideband element and is designed using a multifrequency phase matching method. A single layered dualband reflectarray operating in the 10.7-12.7 GHz band in vertical polarization and the 12.7-14.7 GHz band in horizontal polarization has been proposed [17]. The reflectarray is wideband because of its subwavelength rectangular grids. All of these reflectarrays have wideband or multiband performances but their 1-dB bandwidth is not over 30%.

However, 3D printed reflectarrays have received much attention in recent years [18], [19]. Three-dimensional printed arrays have numerous advantages, such as high flexibility, stable angular response, and outstanding filtering performance compared with their planar counterparts [20]-[22]. One of the advantages to be expected for 3D printed arrays is wideband performance. According to an antenna theory, it is well known that the bandwidth of antennas or scatterers and their volume are tradeoff. Therefore, 3D printed reflectarrays are expected to show wideband performance compared with their planar counterparts. For example, our group has already clarified the wideband performance of a log-periodic dipole array (LPDA) as a scatterer [23]. However, the wideband performance of a reflectarray composed of the LPDA has not been clarified to date.

In this letter, a reflectarray composed of a log-periodic dipole array (LPDA) is proposed. A 10×1 reflectarray is designed by the reflection coefficient obtained using MoM. Wideband performance of the reflectarray and its mechanism are clarified via numerical simulations. The 10×1 element reflectarray is fabricated using a 3D printing technology. The performance of the fabricated reflectarray is measured, and the wideband performance of the proposed reflectarray is clarified experimentally. To fairly compare the bandwidth of the proposed reflectarray with conventional reflectarrays, both 1-dB and 3-dB bandwidths are shown. In this letter, the frequency range over which the drop of the bistatic radar cross section (BRCS) from its peak is less than 1-dB and 3-dB is defined as the 1-dB and 3-dB bandwidths, respectively [24].

II. DESIGN AND FABRICATION OF THE REFLECTARRAY

An LPDA structure is shown in Fig.1. A reflectarray composed of the LPDA is designed as follows [23].

H. Ito is with the KDDI Corporation, Japan (e-mail:konno@ecei.tohoku.ac.jp).

K. Konno, Hiroyasu Sato and Q. Chen are with the Department of Electrical and Communications Engineering, Tohoku University, Japan (e-mail:konno@ecei.tohoku.ac.jp).

Manuscript received August 25, 2011; revised March 29, 2012.

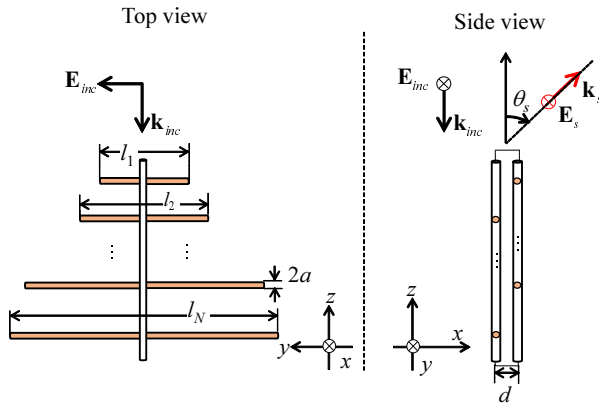


Fig. 1. Reflectarray element.

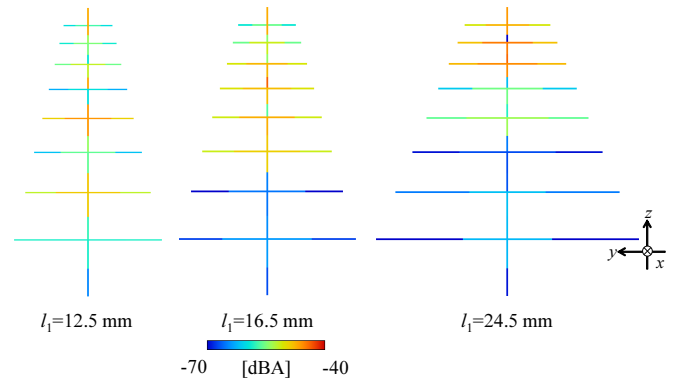


Fig. 3. Current distribution of LPDA elements ($f = 4$ GHz, $s_1 = 5.2$ mm, $\tau = 0.85$, $B_s = 3$, $d = 4$ mm, $a = 0.45$ mm).

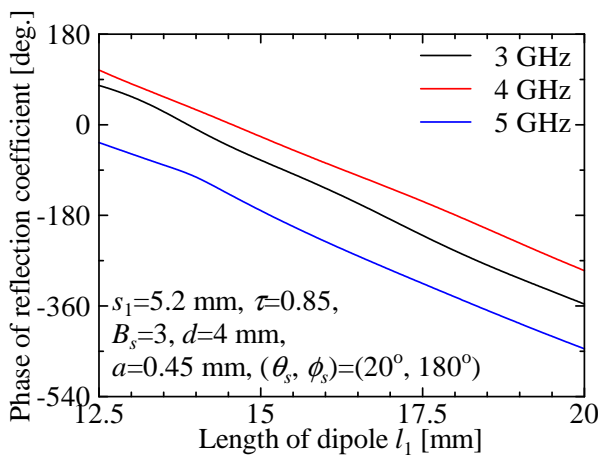


Fig. 2. Phase of reflection coefficient.

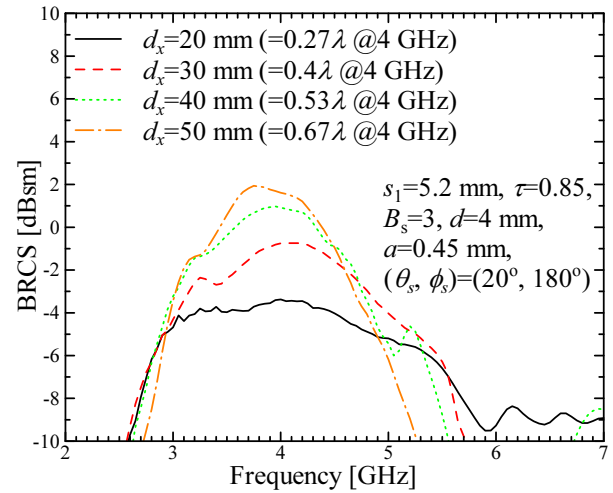


Fig. 4. Simulated BRCS of 10×1 reflectarrays.

- 1) Initial structure parameters of an LPDA, l_1 , s_1 , $B_s = \frac{l_N}{l_1}$, $\tau = \frac{l_{n-1}}{l_n} = \frac{s_{n-1}}{s_n}$, and $N = \lceil 1.5 + \frac{\log B_s}{\log \frac{1}{\tau}} \rceil$ are given. During design process, l_1 is incremented, while s_1 , B_s , τ , and N are fixed.
- 2) The LPDA is illuminated by a plane wave of normal incidence, and the LPDA reflection coefficient is obtained using the MoM. Then, l_1 is incremented, and the reflection coefficient of the LPDA is iteratively obtained. Finally, the reflection coefficient of the LPDA is obtained as a function of l_1 . During the numerical simulation, the LPDA is isolated, and mutual coupling between LPDAs is neglected [25].
- 3) Using the reflection coefficient of the LPDA, the dimensions of each LPDA in a reflectarray is obtained to form a planar phase front to the mainbeam direction.

The phase of the reflection coefficient of an LPDA is shown in Fig. 2. The reflection coefficient was calculated using far field in $(\theta_s, \phi_s) = (20^\circ, 180^\circ)$. It is found that the phase of the reflection coefficient varies smoothly and linearly as l_1 increases. Moreover, a phase range of more than 360° is achieved at every frequency. Linear and smooth phase variations of the reflection coefficient indicate that a fabricated reflectarray using the LPDA is robust for fabrication error. To

clarify why the LPDA has such outstanding performance as a reflectarray element, the current distribution of the LPDA is shown in Fig. 3. It is found that the so-called active region shifts to a forward part of the LPDA as l_1 increases. It is well-known that the active region smoothly shifts when the LPDA works as a frequency-independent antenna. Therefore, Fig. 3 implies that the scattering performance of the LPDA can be wideband in analogy with its radiation performance, i.e., the LPDA works as a wideband reflectarray element because of its self-complementary structure. Linear and smooth phase variations of the reflection coefficient also come from its self-complementary structure. However, it has been clarified that the scattering performance of the LPDA is not as wideband as its radiation performance [23]. This is because when the LPDA works as a scatterer, it has two different current modes excited by plane waves, either directly or via the parallel two wire transmission line. The current mode excited via the parallel two wire transmission line only contributes to the wideband scattering performance of the LPDA because the current mode comes from its self-complementary structure. The current mode excited by the plane wave directly degrades the bandwidth of the LPDA because the current mode is independent of its self-complementary structure.

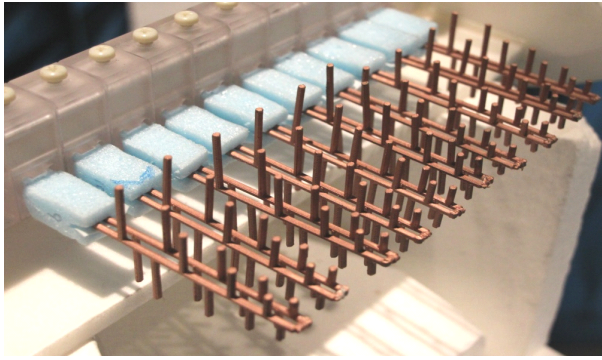


Fig. 5. Fabricated 10×1 reflectarray ($d_x = 20$ mm).

Using the LPDA element, 10×1 reflectarrays were designed at 4 GHz. All structure parameters of the designed reflectarrays are the same as those shown in Fig. 2, except for l_1 . Designed reflectarrays are H-plane arrays; their array spacing is d_x [mm]. To clarify the wideband performance of the designed reflectarrays, simulated BRCS patterns are shown in Fig. 4. It is found that the bandwidth of reflectarrays decreases as their array spacing increases. However, their 3-dB bandwidth is still wide and is more than 30%, even when their array spacing is relatively large (e.g., $d_x = 50$ mm). As mentioned previously, the LPDA works as a wideband reflectarray element because of its self-complementary structure. As a result, the designed reflectarrays are wideband compared with those composed of conventional planar elements that suffer from their inherent narrow bandwidth.

The designed reflectarray was fabricated using a 3D printing technology and was coated by ink made with copper. The fabricated 10×1 reflectarray is shown in Fig. 5.

III. MEASUREMENT RESULTS

A BRCS pattern of the fabricated 10×1 reflectarray was measured in a radio anechoic chamber. Double-ridged waveguide horn antennas (Schwarzbeck BBHA9120D) were used for transmitting/receiving antennas. Because of the limitation of the measurement system, it was difficult to deploy the reflectarray in the far field region of both transmitting/receiving antennas. Therefore, the distance between the fabricated reflectarray and transmitting/receiving antennas was as long as possible but was not sufficiently long to reach the far field region during the measurement.

The measured BRCS pattern of the fabricated reflectarray is shown in Fig. 6. A simulated BRCS pattern using MoM is also shown in Fig. 7. It is shown that the BRCS pattern obtained from measurement and simulation has good agreement. The measured BRCS pattern shows that the fabricated reflectarray forms a mainbeam to the desired direction $(\theta_s, \phi_s) = (20^\circ, 180^\circ)$ over the wideband. A beam squint of the BRCS pattern is seen as a result of the effect of the mutual coupling between reflectarray elements. The beam squint over the entire bandwidth can be minimized by designing a reflectarray using an optimization technique [11]. As shown in Figs. 6 and 7, the measured BRCS is larger than the simulated BRCS. Generally, the measured BRCS is smaller than that of the

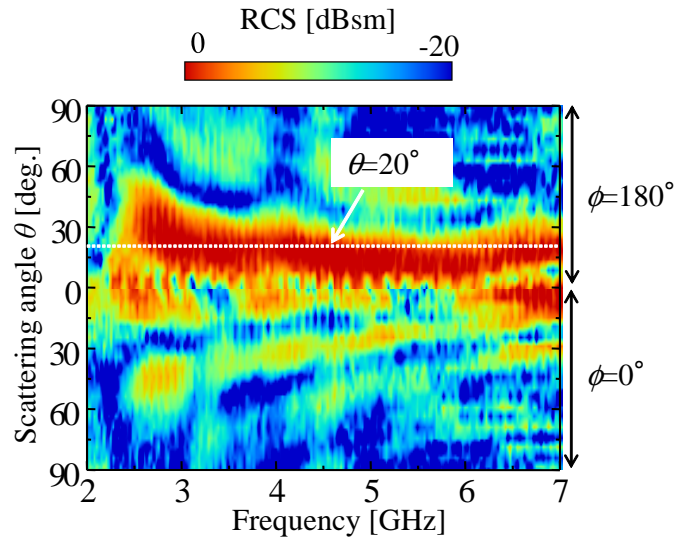


Fig. 6. Measured BRCS pattern.

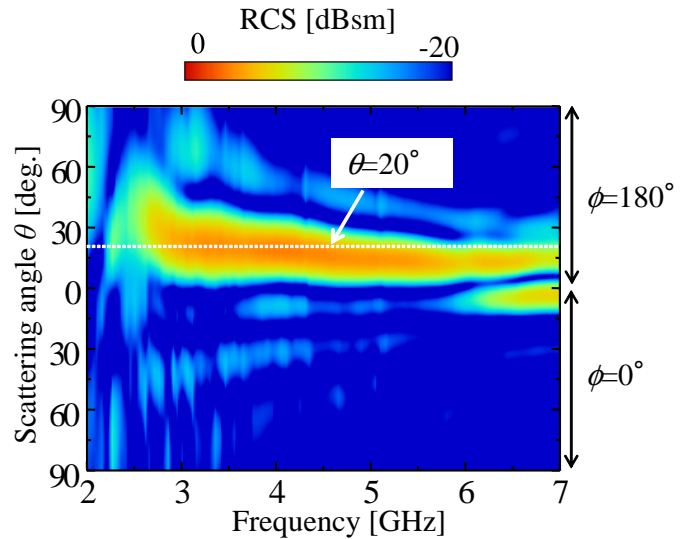


Fig. 7. Simulated BRCS pattern.

simulated one because conductive loss and surface roughness were not considered in the simulation model. However, in our measurement, the distance between the reflectarray and the transmitting/receiving antennas was not long enough to satisfy the far field criterion. The measurement error should have been removed if our measurement system were improved.

The 1-dB and 3-dB bandwidth of the simulated BRCS is 45% (3.1 GHz-4.6 GHz) and 64% (2.8 GHz-5.45 GHz), respectively. It is difficult to evaluate the 1-dB and 3-dB bandwidths of the measured BRCS pattern because the measured BRCS pattern shows a ripple due to the effect of the near field and small receiving signal levels. However, as shown in Figs. 6 and 7, it is clarified that the measured BRCS pattern is similar to the simulation. Therefore, it can be concluded that the measured BRCS pattern also shows the same bandwidth, except for these measurement problems.

IV. CONCLUSION

In this letter the wideband scattering performance of a reflectarray that is composed of an LPDA was shown numerically and experimentally. The reflection coefficient and current distribution of the isolated LPDA were obtained using MoM. Numerical simulation clarified that the wideband scattering performance of the LPDA comes from its self-complementary structure. A 10×1 reflectarray was numerically designed and fabricated using 3D printing technology. The BRCS pattern of the fabricated reflectarray was measured in a radio anechoic chamber. Except for beam squint and the near field effect, it can be said that the wideband scattering performance of our designed reflectarray was verified both numerically and experimentally.

ACKNOWLEDGMENT

We would like to thank staffs in Cyberscience Center, Tohoku University for their helpful advices. This work was financially supported by JSPS KAKENHI Grant Number 25420394 and 26820137, and JSPS Postdoctoral Fellowships for Research Abroad.

REFERENCES

- [1] D.G. Berry, R.G. Malech, and W.A. Kennedy, "The Reflectarray Antenna," *IEEE Trans. Antennas Propag.*, vol.11, no.6, pp.645-651, Nov. 1963.
- [2] J. Huang, "Analysis of a microstrip reflectarray antenna for microspacecraft applications," TDA Progress Report 42-120, Feb. 1995, pp. 153-173.
- [3] J. Huang and J.A. Encinar, *Reflectarray Antennas*, John Wiley and Sons, 2008.
- [4] J.A. Encinar, L.S. Datashvili, J.A. Zornoza, M. Arrebola, M.S.-Castaner, J.L. Besada-Sanmartin, H. Baier, and H. Legay, "Dual-polarization dual-coverage reflectarray for space applications," *IEEE Trans. Antennas Propag.*, vol. 54, no. 10, pp. 2827-2837, Oct. 2006.
- [5] J.A. Encinar, M. Arrebola, L.F. de la Fuente, and G. Toso, "A transmit-receive reflectarray antenna for direct broadcast satellite applications," *IEEE Trans. Antennas Propag.*, vol. 59, no. 9, pp. 3255-3264, Sept. 2011.
- [6] L. Li, Q. Chen, Q. Yuan, K. Sawaya, T. Maruyama, T. Furuno, and S. Uebayashi, "Novel broadband planar reflectarray with parasitic dipoles for wireless communication applications," *IEEE Antennas Wireless Propag. Lett.*, vol. 8, pp. 881-885, 2009.
- [7] L. Li, Q. Chen, Q. Yuan, K. Sawaya, T. Maruyama, T. Furuno, and S. Uebayashi, "Frequency selective reflectarray using crossed-dipole elements with square loops for wireless communication applications," *IEEE Trans. Antennas Propag.*, vol. 59, no. 1, pp. 89-99, Jan. 2011.
- [8] J.A. Encinar and J.A. Zornoza, "Broadband design of three-layer printed reflectarrays," *IEEE Trans. Antennas Propag.*, vol. 51, no. 7, pp. 1662-1664, July 2003.
- [9] J.A. Encinar and J.A. Zornoza, "Three-layer printed reflectarrays for contoured beam space applications," *IEEE Trans. Antennas Propag.*, vol. 52, no. 5, pp. 1138-1148, May 2004.
- [10] M.R. Chaharmir, J. Shaker, M. Cuhaci and A. Ittipiboon, "Broadband reflectarray antenna with double cross loops," *Electron. Lett.*, vol. 42, no. 2, pp.65-66, Jan. 2006.
- [11] M.R. Chaharmir, J. Shaker, and H. Legay, "Broadband design of a single layer large reflectarray using multi cross loop elements," *IEEE Trans. Antennas Propag.*, vol. 57, no. 10, pp. 3363-3366, Oct. 2009.
- [12] M.R. Chaharmir, J. Shaker, and H. Legay, "Dual-band Ka/X reflectarray with broadband loop elements," *IET Microw. Antennas Propag.*, vol. 4, no. 2, pp. 225-231, Feb. 2010.
- [13] M.R. Chaharmir, J. Shaker, N. Gagnon, and D. Lee, "Design of broadband, single layer dual-band large reflectarray using multi open loop elements," *IEEE Trans. Antennas Propag.*, vol. 58, no. 9, pp. 2875-2883, Sept. 2010.
- [14] Q.-Y. Chen, S.-W. Qu, J.-F. Li, Q. Chen, and M.-Y. Xia, "An X-band reflectarray with novel elements and enhanced bandwidth," *IEEE Antennas Wireless Propag. Lett.*, vol. 12, pp. 317-320, 2013.
- [15] T. Smith, U. Gothelf, O.S. Kim, and O. Breinbjerg, "An FSS-backed 20/30 GHz circularly polarized reflectarray for a shared aperture L- and Ka-band satellite communication antenna," *IEEE Trans. Antennas Propag.*, vol. 62, no. 2, pp. 661-668, Feb. 2014.
- [16] S.-W. Qu, H.-X. Zhang, W.-W. Wu, P.-F. Li, S. Yang, and Z.-P. Nie, "Wideband folded reflectarray using novel elements with high orthogonal polarization isolation," *IEEE Trans. Antennas Propag.*, vol. 64, no. 7, pp. 3195-3200, July 2016.
- [17] L. Guo, P.-K. Tan, and T.-H. Chio, "Single-layered broadband dual-band reflectarray with linear orthogonal polarizations," *IEEE Trans. Antennas Propag.*, vol. 64, no. 9, pp. 4064-4068, Sept. 2016.
- [18] P. Nayeri, M. Liang, R.A. Sabory-Garcia, M. Tuo, F. Yang, M. Gehm, H. Xin, and A.Z. Elsherbeni, "3D printed dielectric reflectarrays: low-cost high-gain antennas at sub-millimeter waves," *IEEE Trans. Antennas Propag.*, vol. 62, no. 4, pp. 2000-2008, April 2014.
- [19] H. Yi, S.-W. Qu, K.-B. Ng, C.H. Chan, and X. Bai, "3-D printed millimeter-wave and terahertz lenses with fixed and frequency scanned beam," *IEEE Trans. Antennas Propag.*, vol. 64, no. 2, pp. 442-449, Feb. 2016.
- [20] I.G. Lee and I.P. Hong, "3D frequency selective surface for stable angle of incidence," *Electron. Lett.*, vol. 50, no. 6, pp. 423-424, March 2014.
- [21] B. S.-Izquierdo and E.A. Parker, "3-D printing of elements in frequency selective arrays," *IEEE Trans. Antennas Propag.*, vol. 62, no. 12, pp. 6060-6066, Dec. 2014.
- [22] X.G. Huang, Z. Shen, Q.Y. Feng, and B. Li, "Tunable 3-D Bandpass Frequency-Selective Surface With Wide Tuning Range," *IEEE Trans. Antennas Propag.*, vol. 63, no. 7, pp. 3297-3301, July 2015.
- [23] K. Yokokawa, K. Konno, and Q. Chen, "Scattering performance of log-periodic dipole array," *IEEE Antennas Wireless Propag. Lett.*, (In press).
- [24] C.A. Balanis, "Fundamental parameters of antennas," in *Antenna Theory: Analysis and Design*, 3rd ed. p. 70, Hoboken, NJ, USA: Wiley-Interscience, 2005.
- [25] F. Venneri, G. Angiulli, and G. Di Massa, "Design of microstrip reflectarray using data from isolated patch analysis," *Microw. Optical Technol. Lett.*, vol.34, no.6, pp.411-414, Sept. 2002.